

**ORIGINAL
RESEARCH**

T. Richards
J. Stevenson
J. Crouch
L.C. Johnson
K. Maravilla
P. Stock
R. Abbott
V. Berninger

Tract-Based Spatial Statistics of Diffusion Tensor Imaging in Adults with Dyslexia

BACKGROUND AND PURPOSE: Diffusion tensor imaging is a tool that can be used to study white matter microstructure in dyslexia. We tested the hypothesis that dyslexics have a white matter structural change (as measured by directional diffusion of water, which can be affected by disruption in white matter tracts) between brain regions that previous functional connectivity studies showed were associated with phonologic processing.

MATERIALS AND METHODS: Diffusion tensor imaging (DTI) scans were acquired from 7 healthy adult normal readers and from 14 adults with dyslexia on a 1.5T scanner. Voxelwise statistical analysis of the fractional anisotropy data were carried out by using Tract-Based Spatial Statistics to compare dyslexic subjects versus control subjects in white matter tracts.

RESULTS: Significant group difference map clusters (comparing adults with and without dyslexia) occurred in specific bilateral white matter tracts within the frontal lobe, temporal lobe, occipital lobe, and parietal lobe.

CONCLUSION: The DTI fractional anisotropy results in the bilateral white matter showing higher fractional anisotropy in adult control subjects compared with adults with dyslexia (relating to white matter fiber tract integrity) are consistent with our previous functional connectivity results from seed points in the bilateral inferior frontal gyrus.

Diffusion tensor imaging (DTI) is a technique that can be used to study white matter structures (anisotropy) in the human brain.¹ Le Bihan et al² have written a review about the applications of DTI to study abnormalities in a variety of diseases including stroke, multiple sclerosis, dyslexia, and schizophrenia. DTI has recently been used to study language-related neural pathways in normal and impaired readers.¹⁻⁷ Klingberg et al⁵ reported that white matter diffusion anisotropy in the temporoparietal region of the left hemisphere was significantly correlated with reading scores within the reading-impaired group and within the control group in adults. Niogi and McCandliss⁷ used DTI to investigate the association between variation in white matter microstructure and individual differences in reading skill within children. Their results replicate previous findings of strong positive correlations between fractional anisotropy (FA) values in left centrum semiovale, left superior corona radiata, and bilateral anterior corona radiata and standardized reading scores of typically developing children.⁷ Deutsch et al³ investigated the white matter structure in the left temporoparietal region in children with a wide range of reading performance levels by using DTI. They report that the white matter structure measured using FA and coherence index correlated significantly with behavioral measurements of reading, spelling, and rapid naming performance.³

Molko et al⁶ used DTI to study a patient with alexia in his

left visual field resulting from a posterior callosal lesion and demonstrated how DTI can reveal the anatomic bases of a disconnection syndrome by tracking the degeneration of neural pathways and relating it to impaired fMRI activations and behavior. Dougherty et al⁴ used DTI to demonstrate that properties of specific fiber bundles match those of the hypothetical pathways described in the neurologic literature on alexia.

In the present study, we extend past research demonstrating fMRI connectivity differences between adults with and without dyslexia⁸ to test the hypothesis that these adults also differ in DTI structural changes (FA). DTI is an elegant method for measuring white matter structural changes to test for abnormalities in specific language pathways.

Materials and Methods

DTI scans were acquired from 7 healthy adult normal readers and from 14 adults with dyslexia on an Achieva 1.5T scanner (Philips, Best, The Netherlands). Participants were fathers in a family genetics study of dyslexia^{9,10}; only fathers were studied, because they are less likely to compensate than mothers in this family genetics study.¹¹ Informed consent was taken from all of the participants, and the study was approved by the University of Washington human subject committee (application 96-1872-D13).

The 7 right-handed control good readers and 14 right-handed dyslexic subjects were healthy, native English speakers and ranged in age from 30 to 45 years. The sample was drawn from a population that varied in education level, but most had some education beyond high school even if they did not complete a degree. All of the subjects completed a 4-hour phenotyping battery of psychometric measures, including the prorated verbal intelligence quotient (IQ) of the Wechsler Adult Intelligence Scale-Revised (WAIS-R).¹² Measures were selected based on their good reliability and previous research showing that they assessed processes relevant to learning a written language.^{13,14} All of the fathers were parents of at least 1 child who met the research criteria for dyslexia. To be categorized as a good reader, the father did not show any indicator of dyslexia subphenotypes on a

Received November 20, 2007; accepted after revision December 20.

From the Department of Radiology (T.R., J.S., K.M.), Psychosocial and Community Health, School of Nursing (L.C.J.), and Educational Psychology (P.S., R.A., V.B.), University of Washington, Seattle, Wash; School of Medicine (J.C.), Saint Louis University, St Louis, Mo.

This work was supported by grants P50 33812 and HD25858 from the National Institute of Child Health and Human Development.

Paper previously presented at: Annual Meeting of the Organization for Human Brain Mapping, June 10-14, 2007; Chicago, Ill.

Please address correspondence to Todd Richards, Department of Radiology, Box 357115, Room AA010, Health Sciences Building, 1959 NE Pacific, Seattle, WA 98195; e-mail: toddr@u.washington.edu

DOI 10.3174/ajnr.A1007

Table 1: Means, SDs, and values of *t* comparing means on psychological measures for control subjects and adults with dyslexia

Measure	Control		Dyslexia		<i>t</i>
	Mean	SD	Mean	SD	
Word Identification†	106.14	6.47	94.43	13.29	2.19*
Word Attack†	105.29	5.02	91.14	12.43	2.87†
Real Word Reading	101.71	11.60	85.07	9.95	3.42†
Pseudo Word Reading	94.43	18.17	77.07	9.49	2.91†
GORT 3 Reading Accuracy§	14.86	2.61	9.00	4.61	3.10†
GORT 3 Reading Rate§	14.00	2.24	9.00	3.26	3.63†
WRAT 3 Spelling†	103.29	9.20	86.14	13.97	2.92†
WIAT II Spelling†	113.00	12.38	94.85	13.04	3.02†
Non Word Memory	1.09	0.88	0.70	0.67	1.13
RAN Letter	-0.14	0.80	1.60	1.43	-2.97†
RAS Letter/Number	0.10	1.00	2.41	1.51	-3.66†

Note:—WRMT-R word attack indicates the rate of pronouncing pseudowords on a list, Woodcock Reading Mastery Test-Revised; TOWRE sight word efficiency, rate of pronouncing single words on a list, Test of Word Reading Efficiency; TOWRE phonemic decoding efficiency, rate of pronouncing pseudowords on a list, Test of Word Reading Efficiency; GORT 3 accuracy, accuracy of pronouncing words during oral reading of text, Gray Oral Reading Test; GORT 3 rate, rate of pronouncing words during oral reading of text, Gray Oral Reading Test; WRAT 3 spelling and WIAT II spelling, written spelling of dictated words; nonword memory, oral reproduction of aurally presented pseudowords; RAN letter, rate of pronouncing randomly presented letters in rows; RAN letter and number, rate of pronouncing switching letters and numbers presented in rows.

* $P < .05$.

† $P < .01$.

‡ Scores on a scale of mean = 100; SD = 15.

§ Scores on a scale of mean = 10; SD = 3.

|| Z-scores on a scale of mean = 0; SD = 1.

4-hour test battery^{13,14} and did not report any history of ever having reading or writing problems. To be categorized as a father with dyslexia, the father showed indicators of persisting dyslexia: their accuracy and/or rate in oral single pseudoword reading, single real word reading, or passage reading and/or spelling were below the population mean, and at least 1 SD below WAIS-R prorated verbal IQ; they also reported a history of reading and/or spelling problems. Table 1 reports the means and SDs for each measure for the dyslexic subjects and good readers. Woodcock Reading Mastery Test-Revised (WRMT-R)¹⁵ Word Identification and Test of Word Reading Efficiency (TOWRE)¹⁶ Real Word Reading Efficiency assess the accuracy and rate, respectively, of real word reading. WRMT-R Word Attack and TOWRE Phonemic Decoding Efficiency assess the accuracy and rate, respectively, of phonologic decoding. Gray Oral Reading Test³¹⁷ assesses accuracy and rate of oral reading of text.

The fathers did not differ significantly in mean WAIS-R prorated verbal IQ, a measure of ability to reason verbally. The affected fathers were significantly lower than the control fathers on each of the reading, spelling, and rapid automatic naming measures given, except phonologic working memory, for which the difference failed to reach conventional levels of statistical significance (Table 1). These results show that, despite comparable ability to reason verbally, the fathers with dyslexia had failed to develop comparable reading and writing skills and had persistent difficulty in rapidly associating phonologic codes with alphanumeric stimuli.

MR Imaging Acquisition and Analysis

DTI was performed by using a single-shot spin-echo diffusion-weighted echo-planar pulse sequence with 64 sections covering the whole brain at 2.5-mm section thickness (TR/TE = 9500/74 ms; acquisition matrix = 128 × 128). Diffusion MR images were obtained from 32 noncolinear directions with a b-value of 1000 s/mm² along with a $b = 0$ image with no diffusion gradients. Images were processed off-line by using FSL (FMRIB [The Oxford Centre for Functional Magnetic Resonance Imaging of the Brain] Software Library, <http://www.fmrib.ox.ac.uk/fsl>), which included eddy-current compensation, DTIFit to reconstruct diffusion tensors, and FA. DTIFit is FSL software that fits a diffusion tensor model at each voxel of the diffusion images. DTIFit generates the following 3D images at the same

matrix size and resolution as the original diffusion images: V1 (first eigenvector), V2 (second eigenvector), V3 (third eigenvector), L1 (first eigenvalue), L2 (second eigenvalue), L3 (third eigenvalue), mean diffusivity, FA, and S0 (raw T2 signal with no diffusion weighting). Voxelwise statistical analysis of the FA data were carried out by using tract-based spatial statistics (TBSS),¹⁸ part of FSL.¹⁹ First, FA images were created by fitting the diffusion tensor to the raw diffusion data by using (FMRIB Diffusion Toolbox) and then were brain extracted by using brain extraction tool (BET), part of FSL.²⁰ All of the subjects' FA data were then aligned into a common space by using the nonlinear registration IRTK²¹ (Image Registration Toolkit; <http://www.doc.ic.ac.uk/~dr/software>). The mean FA image was then created and thinned to create a mean FA skeleton, which represents the centers of all tracts common to the group. The TBSS method does not need/perform any presmoothing.

In more detail, the coregistration/skeletonization process involves the following steps.¹⁸ First, all of the subjects' FA images are affine-transformed into 1 × 1 × 1 mm³ MNI152 space (a normalized/averaged brain developed by the Montreal Neurological Institute). Second, the transformed FA images are averaged to create a mean FA image. Third, the mean FA is fed into the tract skeleton generation, which aims to represent all of the tracts that are "common" to all of the subjects. The skeleton will represent each such tract as a single line (or surface) running down the center of the tract. To achieve skeletonization, the local surface perpendicular direction is estimated (at all of the voxels in the image), and a nonmaximum suppression in this direction is performed. In other words, a search is made along all of the voxels in the local "tract perpendicular direction," and the voxel with the highest FA is identified as the center of the tract. The estimated tract perpendicular direction is regularized to improve estimation robustness. Fourth, the center of each tract is found by comparing the FA value with the 2 closest neighbors on each side, in the direction of the tract perpendicular. If the FA value is greater than the neighboring values, then the voxel is marked as lying on the skeleton.

Each subject's aligned FA data were then projected onto this skeleton (Fig 1), and the resulting data were fed into voxelwise cross-subject statistics. A randomization procedure (FSL's randomize, Monte Carlo permutation test) was used to perform the group analysis statistics. TBSS group maps were generated for the nonparamet-

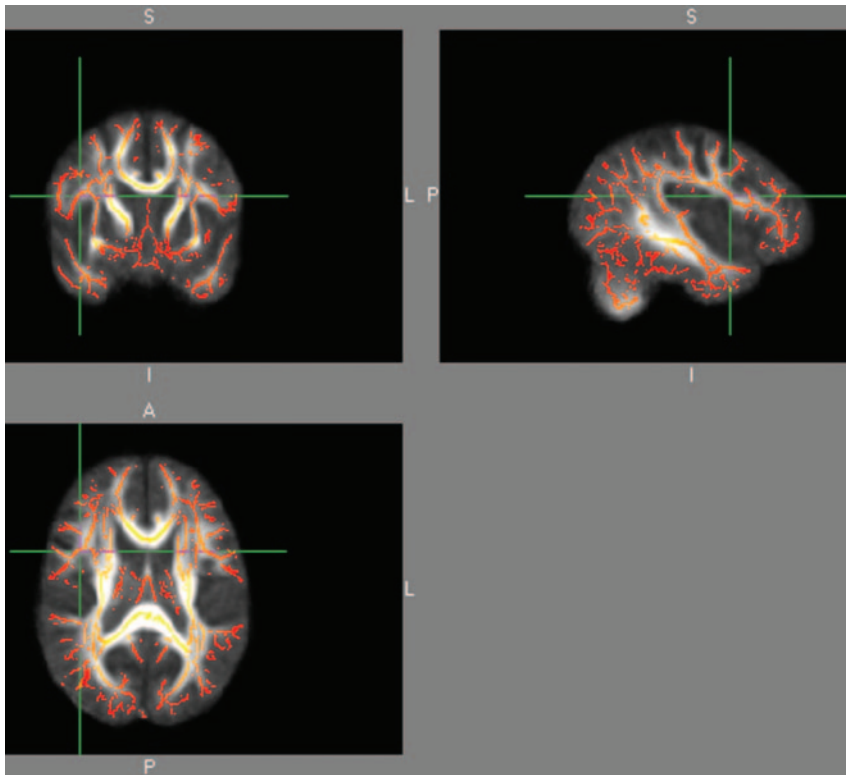


Fig 1. Overlay of skeletonized averaged FA map (orange) onto standardized FA map from DTIs.

ric 2-sample unpaired t test to test whether the control group was greater than dyslexic group and to test whether the dyslexic group was greater than the control group. To perform this nonparametric 2-sample t test, 4D images were created of all of the coregistered skeletonized FA maps (from all of the subjects) and then the following command was executed: “randomize -i TwoSamp4D -o TwoSampT -d design.mat -t design.con -m mask -c 3.” Where TwoSamp4D is the input 4D data of all of the subjects, design.mat contains the design matrix for the GLM model, design.con contains the between group contrast matrix to use with the design matrix, and mask is a brain mask based on FSL’s standard brain mask (avg152_brain_mask.hdr/.img). Randomize produces a test statistic image (eg, tstat1) and sets of P value images (stored as $1 - P$ for more convenient visualization). The $-c 3$ options allowed for cluster-based thresholding (t value threshold of 3 in this case) corrected for multiple comparisons by using the null distribution of the maximum (across the image) cluster size, and the $-c$ options outputs a 3D image showing the exact location of only the significant clusters with zeros everywhere else. All of the statistical output images are in NIFTI GZ (Neuroimaging Informatics Technology Initiative gzipped) format and were viewed and overlaid onto the standard brain using FSLVIEW (FSL software tool). To anatomically define the significant clusters, the DTI maps were coregistered both to the AAL atlas (automated anatomical labeling map which is a 3D map containing 116 brain regions co-registered to standard MNI space developed by Tzourio-Mazoyer et al²²; <http://www.sph.sc.edu/comd/rorden/template.html>) and to a DTI atlas (http://www.loni.ucla.edu/Atlases/Atlas_Detail.jsp?atlas_id = 15). Custom software was written in Fortran to identify the brain region correspondence and MNI (Montreal Neurological Institute) coordinates of each significant cluster.

The authors acknowledge that the TBSS technique has limitations with regard to measuring FA values in regions where there are crossing tracts or tract junctions. Voxelwise statistics are still difficult to

estimate and interpret at tract junctions or crossings. Skeleton continuity is not enforced at junctions, and an artificial lowering of FA value can occur at these junctions or crossing tracts. Another potential confound could have been caused by head motion; however, both dyslexic and control subjects were not different in motion (control \times direction movement in pixels: mean \pm SD = 0.22 ± 0.05 ; dyslexic \times direction movement: mean \pm SD = 0.23 ± 0.045 ; $t = 0.56$; $P = .59$; control y direction movement in pixels: mean \pm SD = 0.31 ± 0.11 ; dyslexic y direction movement: mean \pm SD = 0.30 ± 0.067 ; $t = 0.15$; $P = .88$) as measured by a centroid calculation of the 33 DTI volumes acquired sequentially.

Results

The skeletonized TBSS group map statistical tests showed that control subjects had greater FA compared with dyslexic subjects in many language-related white matter fiber tracts in these adults (Fig 2 and Tables 2 and 3). Significant group difference map clusters occurred in 28 regions located in bilateral white matter tracts within the frontal lobe, temporal lobe, occipital lobe, and parietal lobe (Table 2, as measured from the AAL atlas boundaries). Significant group difference map clusters occurred in an additional 7 regions located in white matter tracts not defined by the AAL atlas (Table 3, as measured from the DTI atlas boundaries).

For test of dyslexic subjects greater than control subjects for the FA value, there were 9 regions with significant clusters (Table 4, as measured from the AAL atlas boundaries). An additional significant group difference map cluster occurred in 1 cerebellar region located in white matter tracts not defined by the AAL atlas (Table 5, as measured from the DTI atlas boundaries). Although some of these regions appear to overlap with the control regions, there were no FA voxels that overlap with the test of control subjects greater than dyslexic

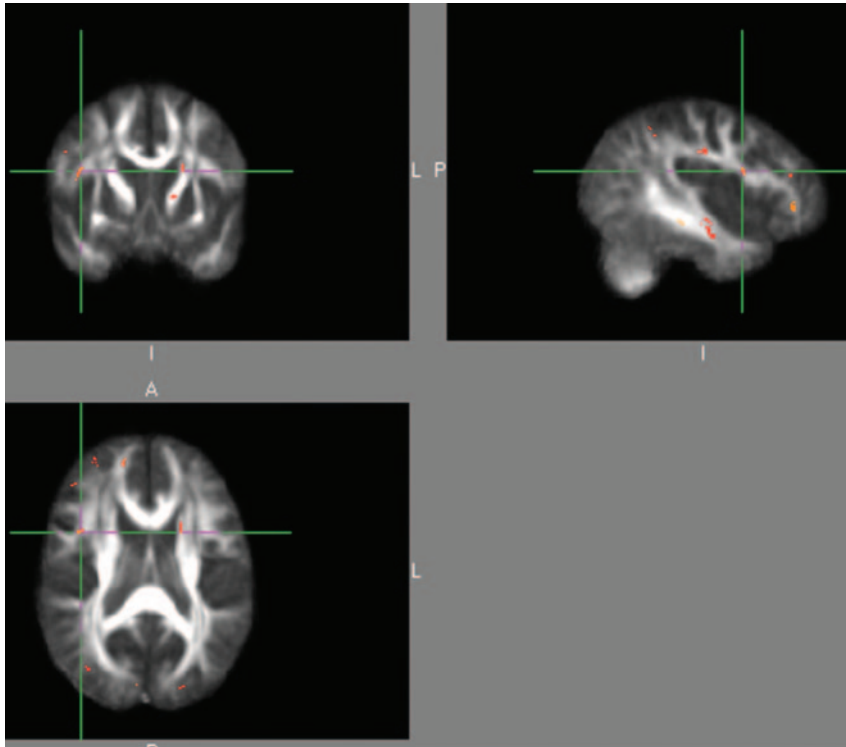


Fig 2. Group difference map for control subjects greater than dyslexic subjects for skeletonized diffusion FA using TBSS software. The crosshair is positioned on a significant cluster near the right inferior frontal gyrus. Orange-red areas show significant clusters for group difference.

subjects. In other words, the clusters for this test are spatially separated from the control greater than dyslexic clusters. The largest clusters were in the cerebellum for this test, and the

control subjects greater than dyslexic subjects had no clusters in the cerebellum.

Software was written to extract individual subject DTI FA

Table 2: White matter regions within the boundaries of the AAL* atlas where control subjects were significantly greater than dyslexic subjects in the skeletonized fractional anisotropy

Brain Region	t Statistic	No. of Voxels	MNI Coordinates†			Brodmann Area	Stanberry Comparison
			x	y	z		
Precentral L	2.55	42	-35	-7	38	6	No
Precentral R	2.94	88	52	0	21	6	No
Frontal Sup R	2.97	54	19	55	17	10	Yes
Frontal Mid R	2.81	45	36	36	17	46	Yes
Frontal Inf Oper R	2.80	86	55	19	0	44	Yes
Frontal Inf Tri R	2.80	38	38	43	1	45	Yes
Frontal Inf Orb L	3.02	60	-47	38	-12	47	No
Frontal Inf Orb R	2.74	91	51	36	-8	47	No
Supp Motor Area R	2.95	44	14	3	61	6	No
Cuneus R	2.89	59	9	-94	12	18	No
Lingual L	2.84	49	-10	-89	-17	18	No
Occipital Sup L	2.77	31	-20	-90	18	18	No
Occipital Sup R	2.78	36	26	-76	26	7	No
Occipital Mid R	2.92	51	42	-77	18	7	Yes
Fusiform L	2.90	21	-20	-84	-19	18	Yes
Fusiform R	2.76	81	41	-11	-32	20	Yes
Postcentral L	3.12	26	-52	-19	30	48	No
Postcentral R	2.53	27	53	-1	22	3	No
Parietal Sup L	3.10	42	-14	-72	47	5	No
Parietal Inf L	2.68	28	-30	-43	45	40	No
Parietal Inf R	3.31	41	47	-47	40	40	Yes
Precuneus L	2.76	16	-10	-72	48	7	No
Putamen L	2.84	32	-17	11	2	0	No
Temporal Sup L	2.69	48	-48	-33	8	22	No
Temporal Pole Sup L	2.88	32	-23	15	-31	38	No
Temporal Mid L	3.08	69	-47	-34	8	39	No
Temporal Inf L	2.79	104	-60	-54	-19	37	Yes
Temporal Inf R	2.57	27	41	-9	-33	20	Yes

Note:—The last column shows the regions where both the current study and Stanberry et al⁹ functional connectivity study have consistency; Sup, superior; Inf, inferior; Orb, orbital; Supp, supplementary; Oper, operculum; L, left; R, right.

*AAL refers to the Automated Anatomical Labeling map which is a 3-dimensional map containing 116 brain regions co-registered to standard MNI space.

† MNI coordinates refers to a standard brain imaging coordinate system developed by the Montreal Neurological Institute.

Table 3: White matter brain regions within the boundaries of the DTI tract atlas regions where control subjects were significantly greater than dyslexic subjects in the skeletonized fractional anisotropy

White Matter Tract Name	<i>t</i> Statistic	No. of Voxels	MNI Coordinates		
			x	y	z
Body of corpus callosum	2.63035	13	-14	-1	36
Anterior limb of internal capsule left	2.88289	48	-17	11	2
Superior corona radiata left	3.11258	11	-16	-4	40
Posterior corona radiata left	2.74872	21	-18	-47	33
Sagittal stratum	2.62251	32	-46	-28	-12
Superior longitudinal fasciculus left	2.70963	55	-37	-23	32
Superior fronto-occipital fasciculus	3.04868	26	-21	9	20

Note:—DTI indicates diffusion tensor imaging; MNI coordinates, standard brain imaging coordinate system developed by the Montreal Neurological Institute.

Table 4: White matter regions within the boundaries of the AAL* atlas where dyslexic subjects were significantly greater than control subjects in the skeletonized fractional anisotropy

Brain Region	<i>t</i> Statistic	No. of Voxels	MNI Coordinates†			Brodmann Areas
			x	y	z	
Precentral L	2.61863	23	-44	8	33	44
Frontal Inf Orb L	2.81102	21	-39	26	-14	47
Fusiform R	2.90205	19	37	-41	-24	37
Postcentral L	2.89957	15	-47	-23	45	3
Temporal Mid L	2.80589	36	-54	2	-32	20
Temporal Mid R	2.84047	16	61	-11	-16	21
Temporal Inf L	2.89029	39	-45	-21	-33	20
Cerebellum R	2.68122	116	41	-60	-39	
Cerebellum L	2.76867	45	-42	-63	-48	

Note:—L, indicates left; R, right; Inf, inferior; Orb, orbital.

* AAL refers to the automated anatomical labeling map which is a 3D map containing 116 brain regions co-registered to standard MNI space.

† MNI coordinates refers to a standard brain imaging coordinate system developed by the Montreal Neurological Institute.

Table 5: White matter brain regions within the boundaries of the DTI tract atlas regions where dyslexic subjects were significantly greater than control subjects in the skeletonized fractional anisotropy

White matter tract name	<i>t</i> Statistic	No. of Voxels	MNI Coordinates		
			x	y	z
Middle cerebellar peduncle	2.796	31	-33	-52	-42

Note:—DTI indicates diffusion tensor imaging; MNI, MNI coordinates, standard brain imaging coordinate system developed by the Montreal Neurological Institute.

and eigen values within a significant cluster near the left inferior frontal gyrus. The results are shown in Table 4. There was a significant difference (*t* test $P < .005$) between the control and dyslexic subjects as tested in these individual FA values in column 2.

Discussion

These results demonstrate white matter differences between adults with and without dyslexia in language-related regions of the brain (see specific region description below). Similar to the results reported by Stanberry et al⁸ that showed stronger functional connectivity in adult control subjects from seed points placed in both bilateral inferior frontal gyri, the current study group also showed differences in the inferior frontal gyri along with several additional brain regions. These results demonstrate DTI structural connectivity that is consistent with the functional connectivity results (Table 2). Common brain regions found across structural and functional connectivity studies include the right superior frontal gyrus, right middle frontal gyrus, right inferior frontal gyrus-operculum, right inferior frontal gyrus-pars triangularis, right middle occipital

gyrus, bilateral fusiform gyri, right inferior parietal, and bilateral inferior temporal gyrus. In contrast to the previous DTI studies of developmental dyslexia that mainly showed differences in left temporoparietal brain regions, the current study reports DTI white matter differences (FA) between adults with

Table 6: DTI FA, eigenvalues for 21 subjects within a significant cluster near the left inferior frontal gyrus (for control subjects greater than dyslexic subjects)

Subject Identification	FA	Eigenvalues × 1e6		
		λL1	λL2	λL3
con 101	4096	1069	642	403
con 105	4180	1016	733	330
con 109	4059	1032	790	337
con 2658	4345	1190	665	440
con 3126	3878	1040	810	369
con 3131	5003	1158	699	359
con 3139	4262	1027	792	379
dys 103	3380	1161	768	549
dys 106	3659	986	744	387
dys 2253	3027	1004	723	503
dys 2254	3225	1102	845	502
dys 2291	3944	957	731	333
dys 2337	3220	1010	828	454
dys 2403	3877	1095	767	411
dys 2418	3033	1034	813	496
dys 2419	3668	1085	824	423
dys 2421	3813	1038	780	389
dys 2506	3746	987	721	387
dys 3021	4686	1122	652	405
dys 3053	3290	1031	790	457
dys 3198	4115	1046	752	410

Note:—DTI indicates diffusion tensor imaging; FA, fractional anisotropy; con, control; dys, dyslexic.

and without dyslexia not only in both temporal regions (fusiform and inferior temporal) but also in right parietal (inferior), right occipital (middle), and many frontal regions.

One possible reason for these reported differences with previous DTI studies is that the current study is the first study that used the new technique of the FSL tractography-based (skeletonized) method for coregistration and group map contrast statistical comparison in the study of dyslexia. However, the main result reported here is consistent with other dyslexia DTI studies (discussed in the introduction) showing lower FA values in white matter in dyslexic subjects compared with control subjects. A possible explanation for the lower FA values in dyslexia is that, in white matter, there could be a less coherent bundle of tracts relating to connectivity of these important language pathways. In other words, the directionality and number of fibers in the white matter may be different in dyslexia and relate to how the water diffuses more readily along the orientation of axonal fibers than in other directions due to obstruction from structural components, such as the myelin sheath. Of particular note is the important change found in the superior longitudinal fasciculus (SLF), which has a role in language. The SLF is composed of 4 distinct components,²³ SLF I, SLF II, SLF III, and arcuate fascicle. SLF III connects the rostral inferior parietal cortex, which receives information from the ventral precentral gyrus. This suggests that the SLF III transfers somatosensory information, such as language articulation, between the ventral premotor cortex, the Brodmann 44 (pars opercularis), the supramarginal gyrus (Brodmann 40), and the lateral inferior prefrontal cortex working memory (Brodmann 46).

Conclusion

The DTI FA results in the bilateral white matter showing higher FA in adult control subjects compared with adults with dyslexia (relating to white matter fiber tract integrity) are consistent with our previous functional connectivity results from seed points in the bilateral inferior frontal gyrus. These DTI findings add to previous MR imaging, functional magnetic resonance spectroscopy, and fMRI connectivity differences found in the right inferior frontal gyrus regions between people with and without dyslexia,²⁴⁻²⁶ which suggest that anomalies at many levels of the brain substrate in this region may contribute to dyslexia. Taken together, these results suggest disconnections in structural, as well as functional, connectivity in the development of dyslexia.

References

1. Stegeman T, Heimann M, Dusterhus P, et al. **Diffusion tensor imaging (DTI) and its importance for exploration of normal or pathological brain development.** *Fortschr Neurol Psychiatr* 2006;74:136–48
2. Le Bihan D, Mangin JF, Poupon C, et al. **Diffusion tensor imaging: concepts and applications.** *J Magn Reson Imaging* 2001;13:534–46
3. Deutsch GK, Dougherty RF, Bammer R, et al. **Children's reading performance is correlated with white matter structure measured by diffusion tensor imaging.** *Cortex* 2005;41:354–63
4. Dougherty RF, Ben-Shachar M, Deutsch G, et al. **Occipital-callosal pathways in children: validation and atlas development.** *Ann NY Acad Sci* 2005;1064:98–112
5. Klingberg T, Hedehus M, Temple E, et al. **Microstructure of temporo-parietal white matter as a basis for reading ability: evidence from diffusion tensor magnetic resonance imaging.** *Neuron* 2000;25:493–500
6. Molko N, Cohen L, Mangin JF, et al. **Visualizing the neural bases of a disconnection syndrome with diffusion tensor imaging.** *J Cogn Neurosci* 2002;14:629–36
7. Niogi SN, McCandliss BD. **Left lateralized white matter microstructure accounts for individual differences in reading ability and disability.** *Neuropsychologia* 2006;44:2178–88
8. Stanberry LI, Richards T, Berninger VW, et al. **Low frequency signal changes reflect differences in functional connectivity between good readers and dyslexics during continuous phoneme mapping.** *Magn Reson Imaging* 2006;24:217–29
9. Raskind W, Hsu L, Berninger V, et al. **Familial aggregation of dyslexic phenotypes.** *Behav Genet* 2000;30:385–96
10. Raskind W, Igo R, Chapman N, et al. **A genome scan in multigenerational families with dyslexia: Identification of a novel locus on chromosome 2q that contributes to phonological decoding efficiency.** *Mol Psychiatry* 2005;10:699–711
11. Raskind WH. **Current understanding of the genetic basis of reading and spelling disability.** *J Learn Disabil Q* 2001;24:141–57
12. Wechsler D. *Wechsler Adult Intelligence Scale-Revised (WAIS-R)*. San Antonio, Tex: Psychological Corporation; 1981
13. Berninger V, Abbott R, Thomson J, et al. **Modeling developmental phonological core deficits within a working memory architecture in children and adults with developmental dyslexia.** *Sci Studies Reading* 2006;10:165–98
14. Berninger V, Abbott R, Thomson J, et al. **Language phenotype for reading and writing disability: A family approach.** *Sci Studies Reading* 2001;5:59–105
15. Woodcock R. *Woodcock Reading Mastery Test - Revised*. Circle Pine, Minn: American Guidance Service; 1987
16. Torgesen J, Wagner R, Rashotte C. *Test of Word Reading Efficiency*. Austin, Tex: ProEd; 1999
17. Wiederholt J, Bryant B. *Gray Oral Reading Test*. 3rd ed. Odessa, Fla: Psychological Assessment Resources; 1992
18. Smith SM, Jenkinson M, Johansen-Berg H, et al. **Tract-based spatial statistics: voxelwise analysis of multi-subject diffusion data.** *Neuroimage* 2006;31:1487–505
19. Smith SM, Jenkinson M, Woolrich MW, et al. **Advances in functional and structural MR image analysis and implementation as FSL.** *Neuroimage* 2004; 23(suppl 1):S208–S219
20. Smith SM. **Fast robust automated brain extraction.** *Hum Brain Mapp* 2002;17:143–55
21. Rueckert D, Sonoda LI, Hayes C, et al. **Non-rigid registration using free-form deformations: application to breast MR images.** *IEEE Trans Med Imaging* 1999;18:712–21
22. Tzourio-Mazoyer N, Landeau B, Papathanassiou D, et al. **Automated anatomical labeling of activations in SPM using a macroscopic anatomical parcellation of the MNI MRI single-subject brain.** *Neuroimage* 2002;15:273–89
23. Makris N, Kennedy DN, McInerney S, et al. **Segmentation of subcomponents within the superior longitudinal fascicle in humans: a quantitative, in vivo, DT-MRI study.** *Cereb Cortex* 2005;15:854–69
24. Richards T, Aylward E, Berninger V, et al. **Individual fMRI activation in orthographic mapping and morpheme mapping after orthographic or morphological spelling treatment in child dyslexics.** *J Neurolinguistics* 2006;19:56–86
25. Richards T, Aylward E, Raskind W, et al. **Converging evidence for triple word form theory in child dyslexia.** *Dev Neuropsychol* 2006;30:547–90
26. Berninger V, Raskind W, Richards T, et al. **A multidisciplinary approach to understanding developmental dyslexia within working-memory architecture: genotypes, phenotypes, brain, and instruction.** *Dev Neuropsychol* 2007; In Press